Int J Adv Manuf Technol (2018) 94:2475–2489
DOI 10.1007/s00170-017-1044-0

ORIGINAL ARTICLE

CEEMDAN and OWMRA as a hybrid method for rolling bearing fault diagnosis under variable speed

Mohamed Lamine Bouhalais[1] · **Abderrazek Djebala**[1] · **Nouredine Ouelaa**[1] · **Mohamed Khemissi Babouri**[1,2]

Received: 17 March 2017 / Accepted: 30 August 2017 / Published online: 11 September 2017
© Springer-Verlag London Ltd. 2017

Abstract The diagnosis of bearing faults in rotating machines working with variable speed, such as wind turbines, gearboxes, and mine excavators, represents a challenge when using vibration analysis. In this paper, the feasibility of an optimized hybrid method based on Empirical Mode Decomposition (EMD) and Wavelet Multi-Resolution Analysis (WMRA) is checked for rolling bearing fault diagnostic by analyzing non-stationary vibration signals obtained from a variable speed rotating machine. An optimized EMD analysis called Complete Ensemble Empirical Mode Decomposition with Adaptive Noise (CEEMDAN) is first used to decompose bearing signals. Amongst obtained Intrinsic Mode Functions (IMF), the one that has the highest kurtosis and covers the bearing natural frequency is chosen to be used for the next step which, given a signal, calculates its envelope by applying Hilbert Transform and then produces a new reconstructed signal using an Optimized WMRA. An Order Tracking (OT) algorithm is then applied on the envelope of the reconstructed signal to remove the effects of speed variation. An envelope order spectrum is finally calculated to bring out the fault characteristic order. The results show that the proposed hybrid approach have successfully highlighted the bearing faults in the non-stationary conditions, with both simulated and experimental signals.

Keywords Vibration analysis · Bearing defects · Variable speed · Empirical mode decomposition · Wavelet multi-resolution analysis · Order tracking · Intrinsic mode function · Hilbert transform

Nomenclature

CEEMDAN	Complete Ensemble Empirical Decomposition with Adaptive Noise
CWT	Continuous Wavelet Transform
DWT	Discrete Wavelet Transform
EMD	Empirical Mode Decomposition
EEMD	Ensemble Empirical Mode Decomposition
FT	Fourier Transform
HT	Hilbert Transform
IMF	Intrinsic Mode Function
MED	Minimum Entropy Deconvolution
MFS	Machine Fault Simulator
OT	Order Tracking
OWMRA	Optimized Wavelet Multi-Resolution Analysis
RMS	Root Mean Square
WMRA	Wavelet Multi-Resolution Analysis
WT	Wavelet Transform
WM	Wavelet Mother

✉ Mohamed Lamine Bouhalais
mouhamed_mars@hotmail.com

Abderrazek Djebala
djebala_abderrazek@yahoo.fr

Nouredine Ouelaa
n_ouelaa@yahoo.fr

Mohamed Khemissi Babouri
babouri_bmk@yahoo.fr

[1] Mechanics and Structures Laboratory (LMS), May 8th 1945 University, Po. Box 401, 24000 Guelma, Algeria

[2] Department of Mechanical Engineering and Productics (CMP), FGM & GP, University of Sciences and Technology Houari Boumediene, Po. Box 32, El-Alia, Bab-Ezzouar, 16111 Algiers, Algeria

1 Introduction

Due to its effectiveness, vibration analysis is being increasingly used for rotating machine surveillance and fault diagnostic. The inspection and analysis of a vibration signal can reveal a lot of information concerning the condition of different machine components, especially for bearings, where one can figure out the presence of faults, their location (outer race, inner race, or ball), and their type (spalls, extended, etc.) [1]. However, for the majority of faults, this information cannot be extracted directly through the visual inspection of signals due to the randomness and the complexity of the physical phenomena responsible of generating them.

In order to overcome this issue, dozens of methods have been invented in a sort of mathematical tools that can be used to derive useful information that help in the process of diagnosis. These tools can be sorted into different categories according to their functional principle: time domain tools, frequency domain tools, or time-frequency tools.

Despite their capability, most of these techniques share a drawback which is that they all have been designed to work with stationary signals measured from constant speed machines, although the industrial development have brought to light a bunch of machines that work with variable speed modes, such as wind turbines, gearboxes, and mine excavators. The necessity of continuous surveillance and diagnostic of that type of machines had put the researchers between two choices: develop new diagnostic tools specifically for that kind of machines, or simply adjust the classical tools to make them useful in this special case.

In the previous literature, we can find that researchers' decisions vary between the two choices; in [2] for example, the traditional tool known as Fourier Transform (FT) which was recognized to be capable of detecting faults in stationary case has been extended to time-varying operation conditions by decomposing the signal over a basis of elementary oscillatory functions whose frequencies follow the speed variations. The result was a new efficient tool called Speed Transform able to detect faults characteristic frequencies under linear speed variations.

Scalar indicators have been proposed in some works, such as [3] where Root Mean Square (RMS) has been used as an indicator to monitor bearing state under variable speed; the vibration signal is acquired simultaneously with a signal from an optical encoder; the instantaneous speed has then been estimated from the signal delivered by the optical encoder. The vibration signal is divided by its corresponding instantaneous speed sample. The RMS value is finally applied to the resulting signal. The state of the bearing has been found to be correlated with the proposed RMS value, which means that we can use this method to figure out whether the bearing is defective or not, but we still cannot localize the fault.

The high efficiency of the known Empirical Mode Decomposition (EMD) method under steady-state regime has led the researchers to test it in the non-stationary case, as in [4], where the bearing fault characteristics have been successfully extracted from the time-frequency envelope spectra of the vibration signal constructed using EMD and instantaneous frequency normalization.

Despite its efficiency, the users of EMD has faced the mode mixing issue, where they may find that different scales may be consisted in one Intrinsic Mode Function (IMF), or that similar scales may reside in different IMFs, which could make individual IMF devoid of physical meaning and lead to false diagnostic [5]. Thus, a new version of EMD called Ensemble Empirical Mode Decomposition (EEMD) was proposed and used since then [5]. The EEMD consists in calculating an ensemble of trials using the original EMD after the addition of white noise. The mean of the result of each ensemble represents the true IMF. In this case, the accuracy of the result is relative to the chosen number of ensembles; more ensembles mean more accuracy, but more time to wait, which could be considered as a drawback.

In [6], the authors presented an optimized EEMD algorithm that, comparing with the classical EEMD, requires less than half iterations to determine all the IMFs. The key idea on the new tool relies on adding a particular noise at each stage of decomposition and a unique residue is computed to obtain each mode. The new method named Complete Ensemble Empirical Mode Decomposition with Adaptive Noise (CEEMDAN) has been tested with electrocardiogram signals and proven to be effective with non-linear and non-stationary signals.

For more efficiency, EMD and its optimized versions are often combined with other techniques. In [7], for example, a hybrid method based on EEMD and Spectral Kurtosis is used to recover faulty bearing signals from large noise. In [8], the Minimum Entropy Deconvolution (MED) is combined with EMD and Teager Kaiser Energy Operator (TKEO) in order to demodulate acoustic and vibration signals which is a key operation for diagnosing bearing faults. In [9], EMD and EEMD are used as a hybrid approach for misalignment diagnosis. In dozens of papers, EMD was used together with artificial intelligence tools in order to automate the diagnosis process of rotating machine faults including bearing faults; the works [10, 11] could be considered as examples. In [12] EMD was applied on wavelet denoised vibration signals for the diagnosis of roller bearing faults. The co-authors of this paper have previously proved that a hybrid method consisted of EMD and WMRA get better time and frequency domain visualization of the fault occurrence in steady-state regime compared to the application of WMRA or EMD alone [13].

In this paper, CEEMDAN is tested together with WMRA for the analysis of non-stationary bearing signals measured under variable speed. First, CEEMDAN will be used to decompose bearing signals into Intrinsic Mode Functions (IMF). The IMF having the highest kurtosis and covering the bearing

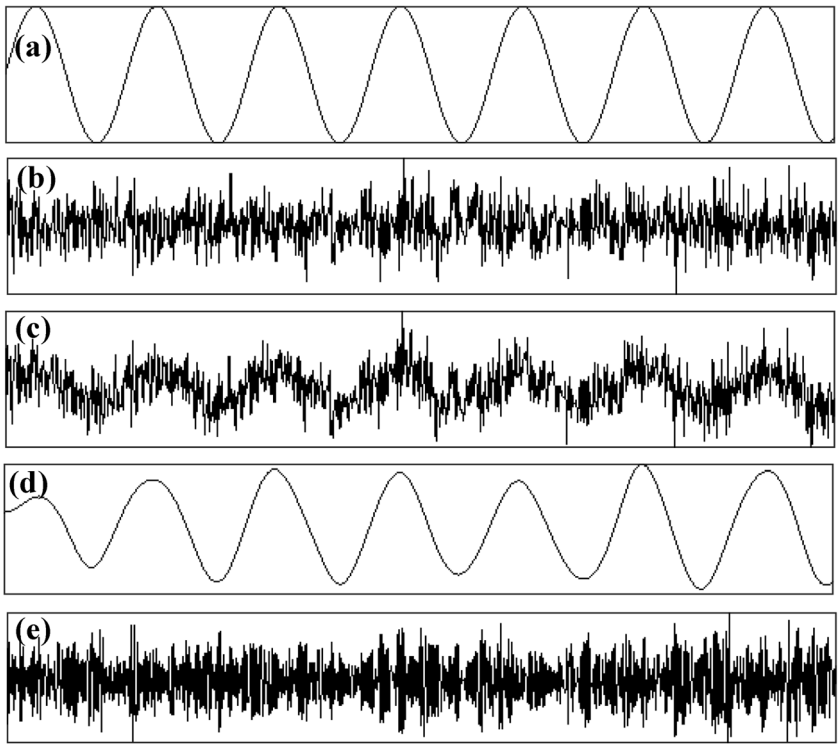

Fig. 1 Simulated signals: a) sine signal, (b) noise signal, (c) sum of sine + noise signals, (d) sine IMF, e) noised IMF

natural frequency is chosen as the optimal one. The envelope signal obtained by applying Hilbert Transform on the optimal IMF is processed by an optimized WMRA to produce a new reconstructed signal. An Order Tracking (OT) algorithm is then applied on the envelope of the reconstructed signal to remove the speed variation effects. An envelope order spectrum is finally performed to highlight the fault order.

2 Complete ensemble EMD with adaptive noise

A complex vibration signal is usually a combination of less-complex signals generated by deferent components of the machine. The EMD is a self-adaptive technique that can be used to decompose any complex signal into a set of signals called IMFs that represent the natural oscillatory modes embedded in that signal. An IMF must satisfy two conditions:

1. In the whole data set, the number of extrema and the number of zero-crossings must either equal or differ at most by one.
2. At any point, the mean value of the envelope defined by the local maxima and the envelope defined by the local minima is zero.

EEMD calculates an ensemble of trials using the original EMD, adding in each trial a different realization of white noise of finite variance. The mean of the result of each ensemble represents the true IMF. This can be summarized as follows [5]:

1. Generate $x^i(t) = x(t) + n^i(t)$, where $x(t)$ is the original signal and $n^i(t)$ [i = 1 ….I] are different realizations of white Gaussian noise
2. Each $x^i(t)$ is decomposed by EMD getting its modes $IMF_k^i(t)$, where $k = 1\ldots$. I indicates the modes,

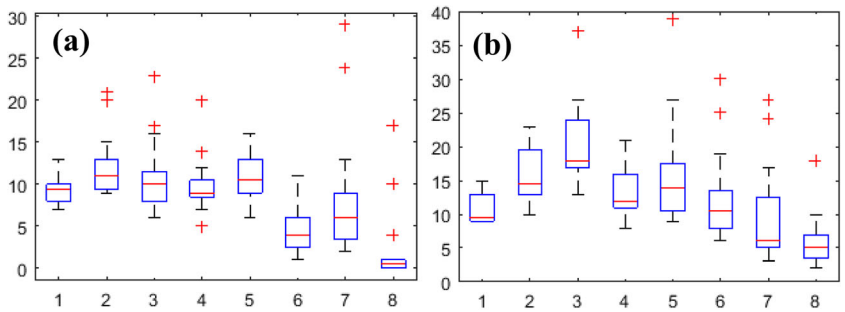

Fig. 2 Number of iterations: (a) CEEMDAN iterations, (b) EEMD iterations

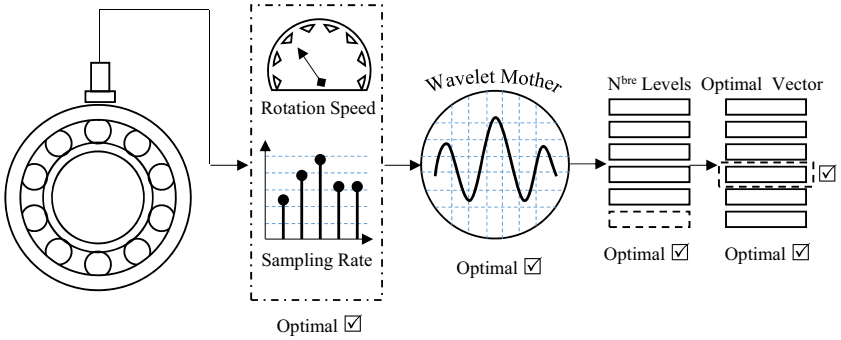

Fig. 3 The OWMRA process

3. Assign $\overline{IMF_k}$ as the k-th mode of $x(t)$, obtained as the average of the corresponding

$$\overline{IMF_k(t)} = \frac{1}{I}\sum_{i=1}^{I} IMF_k^i(t) \tag{1}$$

CEEMDAN uses the same EEMD algorithm to calculate the first mode function $\overline{IMF_1}$ only, a unique first residue is then calculated as [6]:

$$r_1(t) = x(t) - \overline{IMF_1(t)} \tag{2}$$

Then, compute the EMD mode over an ensemble $r_1(t)$ plus different realizations of a given noise obtaining $\overline{IMF_2}(t)$ by averaging. $r_2(t)$ is then calculated as:

$$r_2(t) = r_1(t) - \overline{IMF_2(t)} \tag{3}$$

This step is repeated with the other modes until the stopping criterion is reached.

In order to summarize the procedure of CEEMDAN, $E_j(.)$ is defined as an operator which, given a signal, produces the j-th mode obtained by EMD; ε_i represents the Signal to Noise Ratio (SNR); the steps of the technique are then the following [6]:

1. Decompose I realizations of $x(t) + \varepsilon_0\, n^i(t)$ by EMD to obtain the first $\overline{IMF_1}$ by averaging:

$$\overline{IMF_1(t)} = \frac{1}{I}\sum_{i=1}^{I} IMF_1^i(t) \tag{4}$$

2. Calculate the first residue as:

$$r_1(t) = x(t) - \overline{IMF_1(t)} \tag{5}$$

3. Decompose I realizations of $r_1(t) + \varepsilon_1 E_1(n^i(t))$ until their first EMD mode and calculate the second mode:

$$\overline{IMF_2(t)} = \frac{1}{I}\sum_{i=1}^{I} E_1\left(r_1(t) + \varepsilon_1 E_1\left(n^i(t)\right)\right) \tag{6}$$

4. For $k = 2, \ldots, K$, calculate the k-th residue:
$$r_k(t) = r_{k-1}(t) - \overline{IMF_k(t)} \tag{7}$$

5. For $k = 2, \ldots, K$, define the $(k+1)$-th mode as:
$$\overline{IMF_{k+1}(t)} = \frac{1}{I}\sum_{i=1}^{I} E_1\left(r_k(t) + \varepsilon_k E_k\left(n^i(t)\right)\right) \tag{8}$$

6. Go to step 4 for next k

Steps from 4 to 6 are repeated until the obtained residue in no longer feasible to be decomposed and satisfies:

$$R(t) = x(t) - \sum_{k=1}^{K} \overline{IMF_k}(t) \tag{9}$$

with K as the total number of modes. The original signal $x(t)$ can be expressed in the end as:

$$x(t) = \sum_{k=1}^{K} \overline{IMF_k}(t) + R(t) \tag{10}$$

For more details about CEEMDAN, readers may refer to [6].

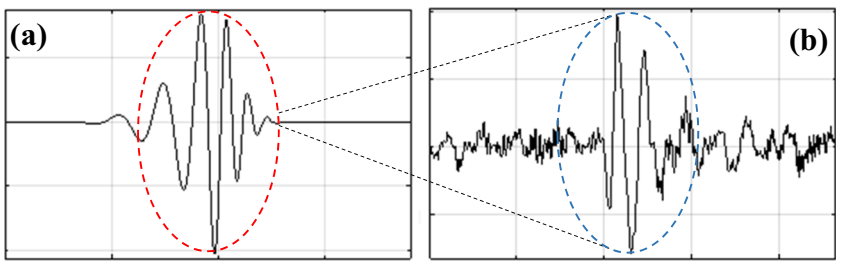

Fig. 4 The similarity between the Daubechis Wavelet (a), and the zoomed shock signal (b)

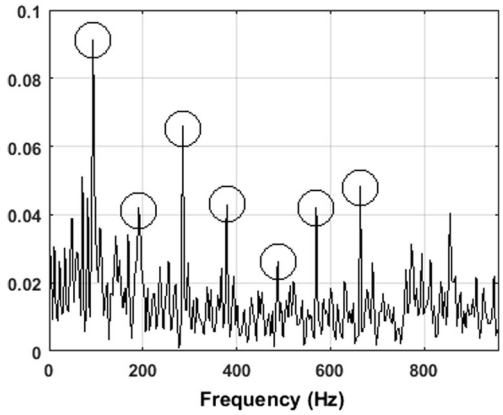

Fig. 5 Faulty bearing's FFT spectrum in case of constant speed

As mentioned previously, the power of CEEMDAN relies on its capability of decomposing signals with less number of iterations comparing with EEMD; this could be verified by a simple test. The noised sinusoidal signal of Fig. 1c is decomposed by both CEEMDAN and EEMD. The result shows that despite the two approaches having successfully separated the sinusoidal signal from the noise Fig. 1d, e, CEEMDAN took less iterations; the total number of needed iterations for EEMD was at about 2345, while it was only 1415 for CEEMDAN as shown in Fig. 2.

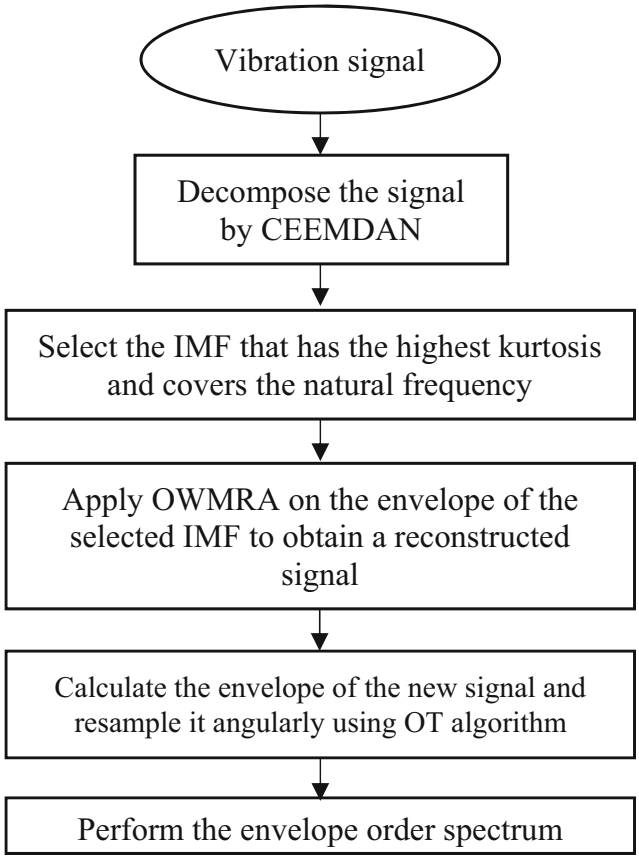

Fig. 7 Flowchart of the proposed method

3 Optimized wavelet multi-resolution analysis

The WMRA is based on the Wavelet Transform (WT), a mathematical transformation which was first used by Morlet [14] in order to overcome the limitations faced when using FT for signal processing. While FT is known as a transformation that decomposes a signal into a weighted set of sine and cosine functions using the concept of the cross-correlation, WT uses the same concept but, instead, represents a signal $x(t)$ in terms of shifted and dilated version of impulse-like singular function called Wavelet Mother (WM), generally represented as a function of zero average:

$$\int_{-\infty}^{\infty} \psi(t)\, dt = 0 \tag{11}$$

which is dilated with a scale parameter a and translated by b

$$\psi_{a,b}(t) = \frac{1}{\sqrt{a}}\psi\left(\frac{t-b}{a}\right) \tag{12}$$

The Continuous Wavelet Transform (CWT) of a signal $x(t)$ is then obtained by the cross-correlation with the conjugate of $\psi(t)$:

$$CWT(a,b) = \frac{1}{\sqrt{a}} \int_{-\infty}^{+\infty} x(t)\psi^*\left(\frac{t-b}{a}\right)dt \tag{13}$$

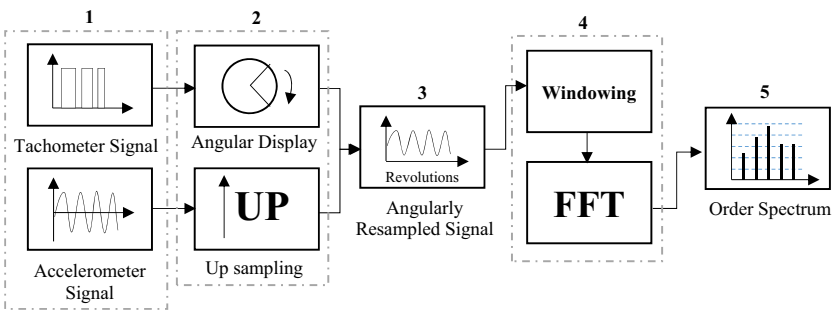

Fig. 6 Order Analysis algorithm

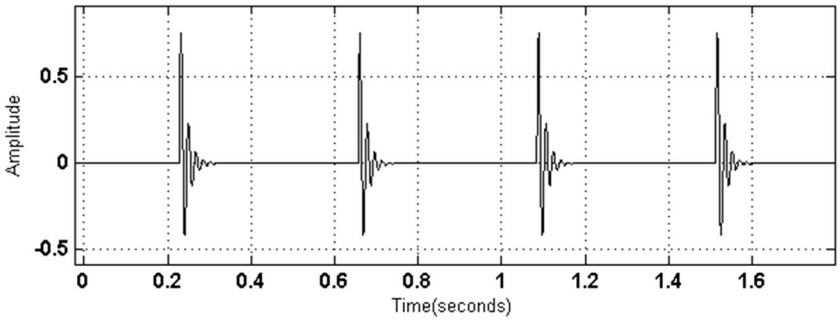

Fig. 8 A simulated signal of a defective bearing working under constant speed

Since measured signals are often digitized, a discretization of the CWT is needed. By replacing a and b by 2^m and $n2^m$, respectively (m and n integers), we can obtain the Discrete Wavelet Transform (DWT); the above expression becomes:

$$DWT(m,n) = 2^{\frac{-m}{2}} \int_{-\infty}^{+\infty} x(t)\psi^*(2^{-m}t-n)dt \tag{14}$$

The complexity of computing the DWT when having a large-scale data led to the introduction of the more practical version known as WMRA by Mallat [15]. The WMRA rapidly computes the DWT by convolving the signal $x(t)$ with low-pass (L) and high-pass (H) filters to obtain two vectors, cA_i and cD_j, representing the low frequencies and the high frequencies of $x(t)$, respectively.

In order to overcome the down sampling experienced during the decomposition, the elements of cA_i and cD_j are passed through two reconstruction filters (LR) and (HR), which give us two new vectors called *approximations* (A_j) and *details* (D_j) with:

$$A_{j-1} = A_j + D_j \tag{15}$$

$$x = A_j + \sum_{i \le j}^{n} D_i \tag{16}$$

with i and j integers.

The WT is widely used for many applications and in different domains. Depending on the desired results, the user have to choose between a lots of disparate parameters such as the WM, the number of decomposition levels, and the

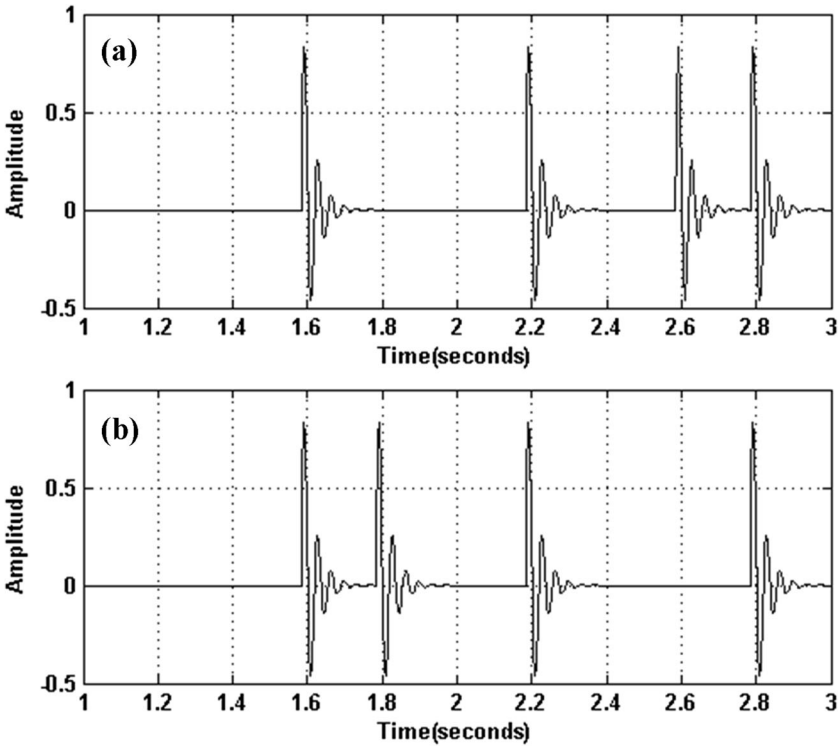

Fig. 9 Fault frequency variation under variable speed: a) acceleration, b) deceleration

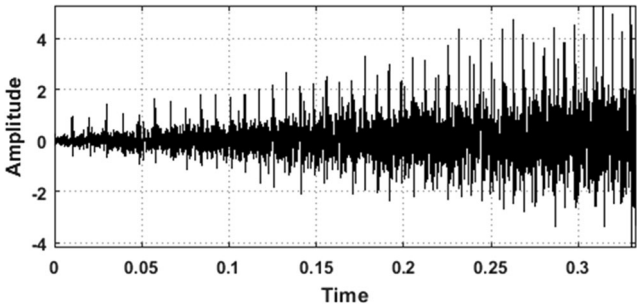

Fig. 10 Simulated bearing signal under variable speed (acceleration)

optimal vector. The idea behind the implementation of an Optimized WMRA (Fig. 3) is that the bearing signal requires a tool specifically adapted to its impulse-like form. In the works [13, 16, 17], it has been found that the results of the application of WMRA on bearing signals are mainly affected by four major parameters:

- The choice of the optimal measurement parameters
- The choice of the optimal analysis wavelet or the WM
- The choice of the optimal number of decomposition levels
- The choice of the optimal decomposition vector

The principal measurement parameters are rotation speed ranges and sampling rate. In previous works [16–19], a relation was found between the measurement parameters and the capacity of the kurtosis which is important for our approach. The ranges of the rotation speed and the values of the sampling rate have to be chosen in a way that guarantees that the shock relaxation time will not exceed the impact repetition period and provoke the loss of the efficiency of the information provided by the kurtosis.

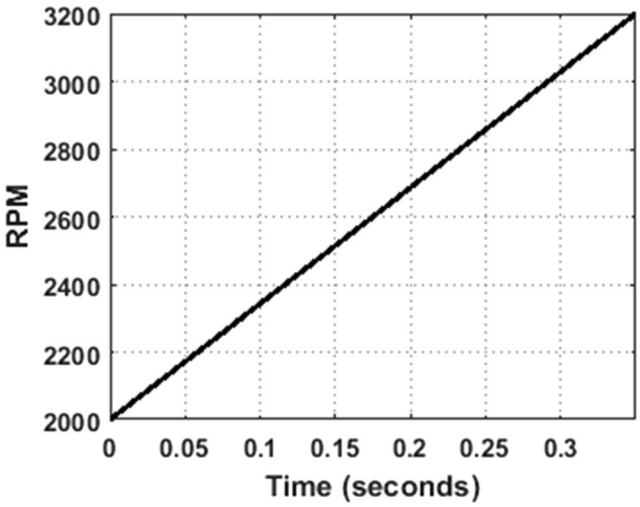

Fig. 11 Speed variation profile for the simulated signal

As mentioned previously, the WT uses the concept of cross-correlation, which is a mathematical way used to look for similarity between two functions. So when used for bearing fault detection, the optimal WM has to be the one that most looks like the shock signal (Fig. 4). It is also proved that the kurtosis can be used as a criterion for this choice since we know that the wavelet that gives the reconstructed signal having the highest kurtosis is the optimal one [16, 17].

In the final step of the OWMRA, we should only preserve the levels which include information. The maximum frequency $F_{max}(A_n)$ of the final level's approximation (A_n) must imperatively contain the shock frequency and at least some of its harmonics in order to confirm that it is indeed the defect frequency. Practically, one considers that three are rather sufficient [16, 17]. Knowing that:

$$F_{max}(A_j) = \frac{F_{max}(x)}{2^j} \tag{17}$$

The maximum frequency of the final level n must thus satisfy

$$F_{max}(A_n) = \frac{F_{max}(x)}{2^n} \geq 3F_{cmax} \tag{18}$$

Therefore, the number of levels must in its turn satisfy

$$n \leq 1.44 log\left(\frac{F_{max}(x)}{3F_{cmax}}\right) \tag{19}$$

The decomposition optimal vector, called reconstructed signal, is the one which allows the defect detection with the best possible resolution, which leads to select the best filtered one. The optimal vector will then be the one having the most significant kurtosis.

4 Order analysis

In constant speed case, the FT is often used to calculate the spectrum of a given signal in order to extract information needed for the diagnosis of machines. A spectrum may reveal shaft speed harmonics, gear meshing frequencies, bearing characteristic frequencies, and other components which may appear depending on the composition and the condition of the machine. Figure 5 represents an envelope spectrum of a raw vibration signal measured from a faulty bearing mounted on a machine fault simulator, the rotation speed has been set to about 30 Hz and the bearing fault characteristic frequency is equal to 92 Hz. The harmonics of the fault characteristic frequency are clearly visible.

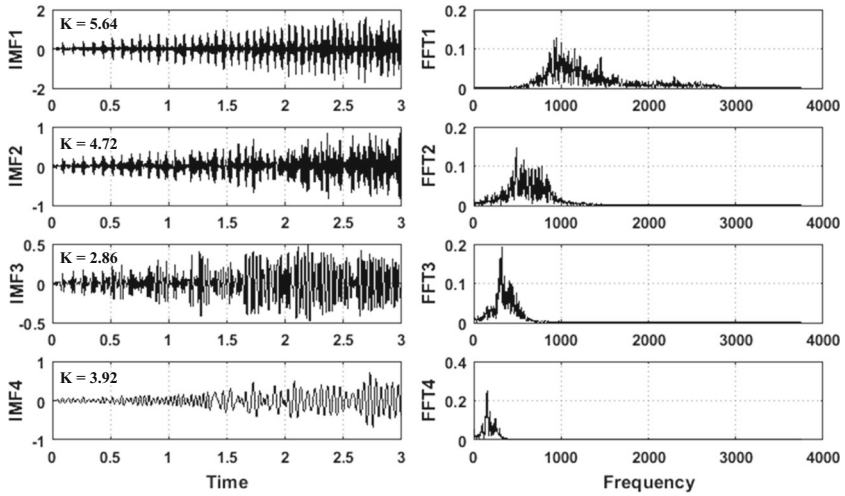

Fig. 12 The obtained IMFs and their corresponding FFTs

When the speed is variable, the majority of signal components follows the speed variation, which makes FT incapable of detecting anything useful since it only detects oscillatory functions whose frequencies are constant. To avoid such a problem, it is often preferred to have a spectrum with *x*-axis based on Orders instead of frequencies as shown in Fig. 6, where orders are just harmonics of shaft speed. The process of diagnosis is then performed by calculating the characteristic orders of machine elements and looking for the corresponding picks in the obtained order spectrum.

The order spectrum is obtained after a succession of mathematical operations that starts by resampling the temporal signal to angular domain using a tachometer signal and ends with the calculation of the FFT. The whole operation is called "Order Tracking" or "Order Analysis" and is often performed as summarized in Fig. 7. More details about this technique could be found in [20–22].

5 The proposed method

The proposed method represented in Fig. 8 can be summarized in the following steps:

The raw signal is decomposed by CEEMDAN into a number of IMFs:

1. The kurtosis and the FFT spectra of all the IMFs are calculated. The IMF having the most important kurtosis and covering the relevant natural frequency is selected.
2. An envelope signal of the selected IMF's energy is calculated from the Hilbert transform.
3. An optimized WMRA is applied on the envelope signal.
4. A reconstructed signal is obtained, from which is calculated a new envelope.
5. Order analysis is performed and an order spectrum highlighting the defect characteristic order is obtained.

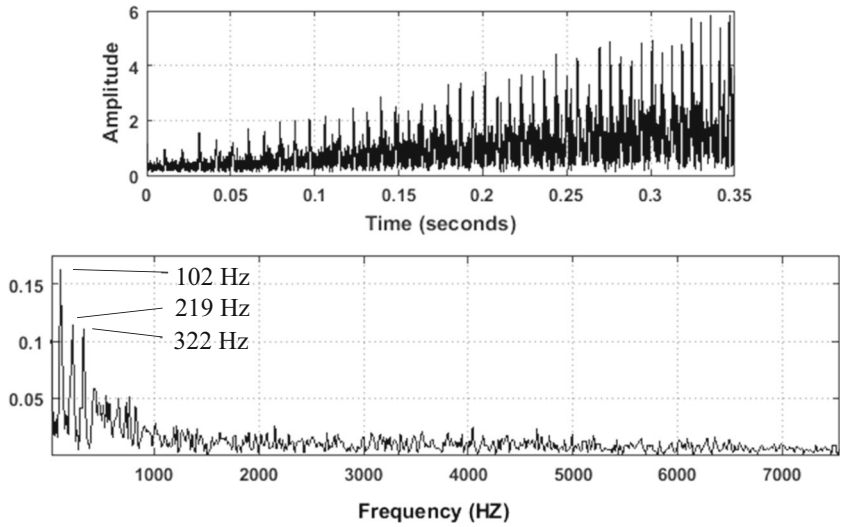

Fig. 13 The envelope of the reconstructed signal with its spectrum

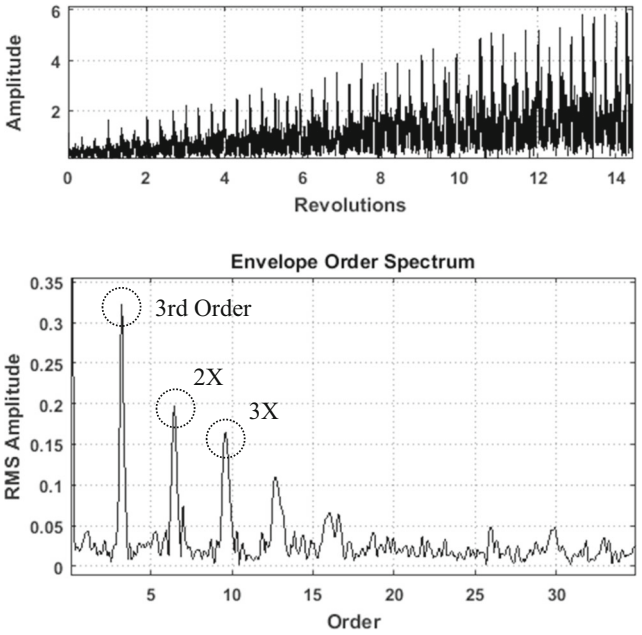

Fig. 14 The angularly resampled envelope with its envelope order spectrum

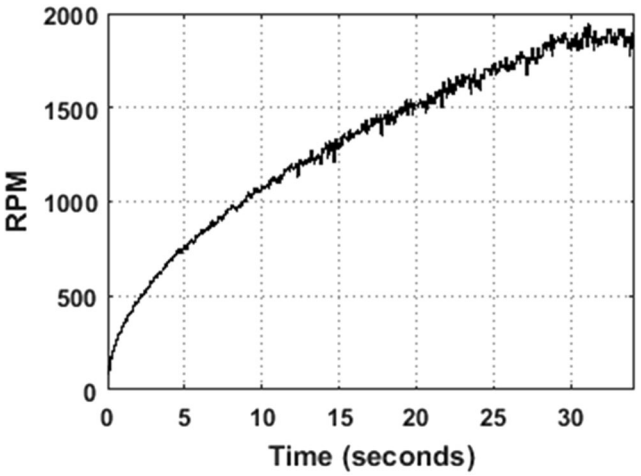

Fig. 16 RPM curve as measured with the tachometer

6 The simulation model

Generally, a complex vibration signal of a faulty bearing can be theoretically decomposed into a number of simple parts. In the case of a single race defect, the main part is the series of impulses generated by the impacts between the rolling elements and the defected race surface, repeated at a certain frequency. The period between two impulses can be determined by calculating the characteristic frequencies of the bearing using a number of equations based on the knowledge of the bearing geometry and the rotation speed as follows [23]:

Ball Pass Frequency Outer Race:

$$BPFO(Hz) = S.C_1 \tag{20}$$

Ball Pass Frequency Inner Race:

$$BPFI(Hz) = S.C_2 \tag{21}$$

Ball Spin Frequency:

$$BSF(Hz) = S.C_3 \tag{22}$$

Fundamental Train Frequency:

$$FTF(Hz) = S.C_4 \tag{23}$$

Where C_1 , C_2 , C_3, and C_4 are constants (which will be later called as Orders) determined from the bearing geometry, and S is the rotation speed.

Thus in the stationary case, the period between the generated impulses is theoretically constant, a simulated signal can be easily constructed knowing that every impulse is an exponentially decaying sinusoid in the form of [23]:

$$s(t) = e^{-\alpha t} sin(2\pi f_r t) \tag{24}$$

where α is the damping ratio of the impulse, and f_r is the bearing resonance frequency.

Fig. 8 represents an example of a simulated signal of a defective bearing working under constant speed.

In the non-stationary case, the fault frequency is variable and follows the speed variation, which means that the period between impulses is unequal. In the case of an acceleration,

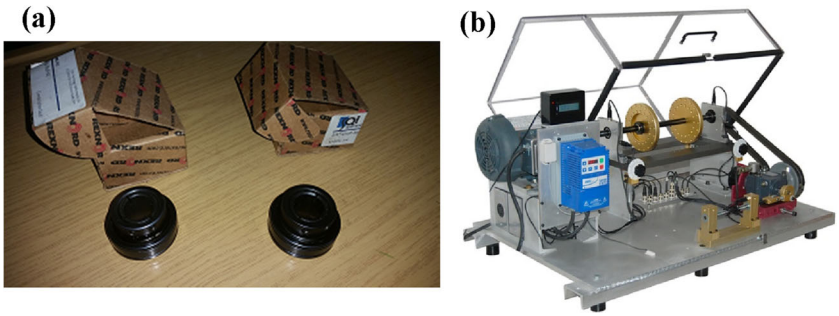

Fig. 15 The used equipment: a) tested bearings, b) MFS

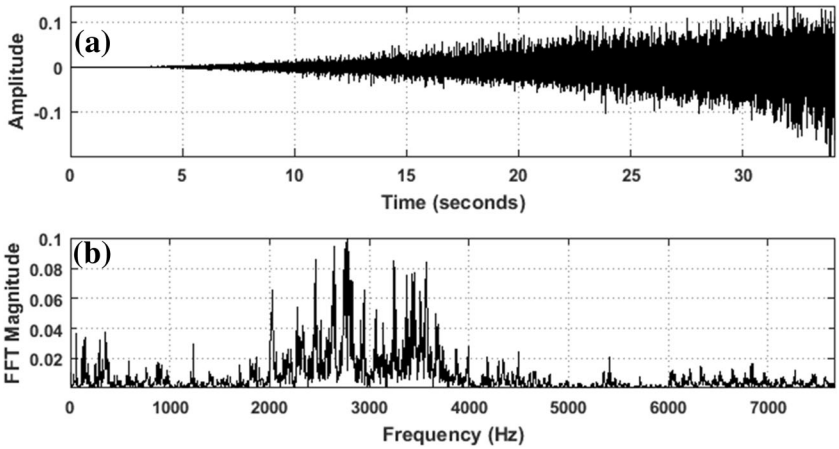

Fig. 17 (a) the measured signal, (b) its corresponding FFT spectrum

the period decreases while speeding up. On the other hand, it increases in the case of deceleration. Examples for both cases are represented in Fig. 11.

In practice, bearing signals are often contaminated with noise and modulated either by shaft speed, cage speed, or their difference, depending on the fault location [24]. It is also often that a time lag between impulses occurred due to the slippage of the rolling elements between the two bearing rings. The final obtained signal can be then mathematically expressed as [24, 25]:

$$x(t) = \sum_i A_i h(n - iT - \tau_i) + n(t) \tag{25}$$

where A_i is the amplitude modulation of the i-th impact force, T is the period between two successive impacts, τ is the time lag produced by the slip, $h(.)$ is the impulse response, and $n(t)$ is the white Gaussian noise. It should be noted that T is variable in the non-stationary case.

The adopted model has been successfully used in the previous works to represent bearing signals [24, 25]. Figure 10 could be considered as an example of the final result obtained by such a model in acceleration case.

7 Application on simulated signal

Before applying the proposed method on real measured signals, it will be tested on simulated signals first; the latter are generated using the model mentioned above. The signal shown in Fig. 10, which simulate a faulty bearing with fixed outer race and rotating inner race, will be analyzed with the proposed method. The fault order is taken equal to 3, and the natural frequency is equal to 850 Hz. The rotation speed is varied from 2000 to 3300 rpm within 0.35 s as shown in Fig. 11.

7.1 First step

The first step of the proposed method is the decomposition of the signal by CEEMDAN. The results of the decomposition

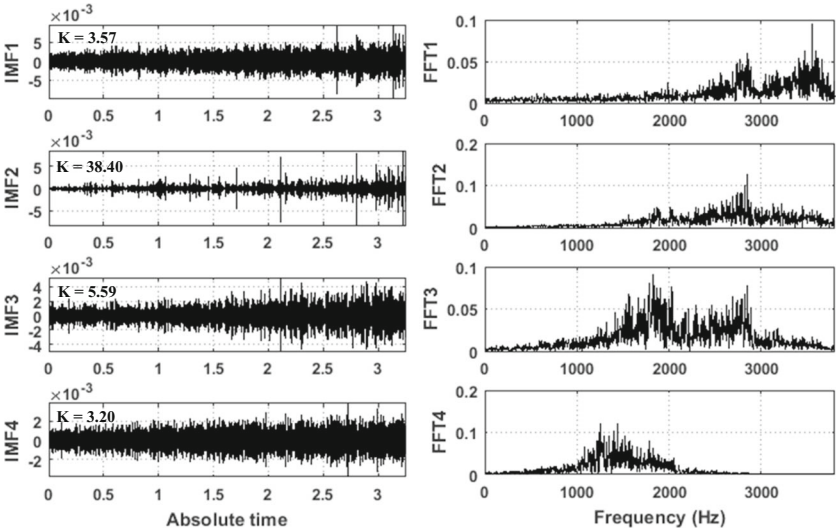

Fig. 18 IMFs of the measured signal with their corresponding FFTs (Outer race fault)

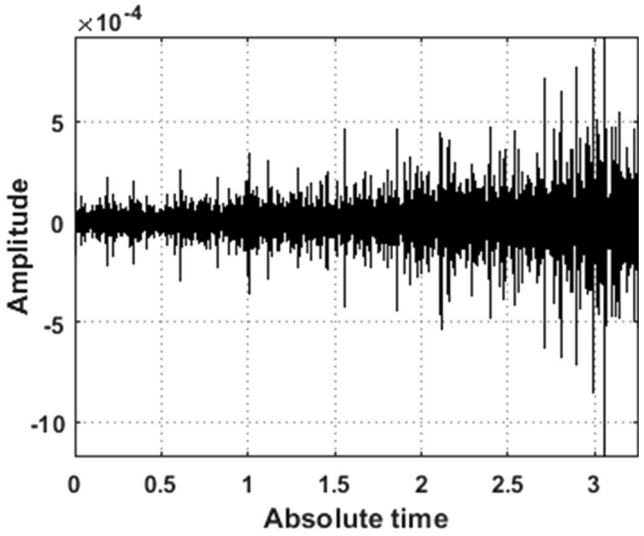

Fig. 19 The reconstructed signal of the chosen IMF envelope

are shown in Fig. 12. According to Fig. 13, the IMF1 appears to be the best IMF to be used for the next step, since it has the most significant kurtosis (5.64) and covers the natural frequency chosen for the simulation (850 Hz).

7.2 Second step

The second step consists in applying OWMRA on the envelope of the selected IMF (IMF1); a reconstructed signal is obtained. As shown in Fig. 13, a classical envelope spectrum does not give anything significant when applied on the reconstructed signal due to the speed conditions. Angular resampling is then applied to remove the effects of speed variation.

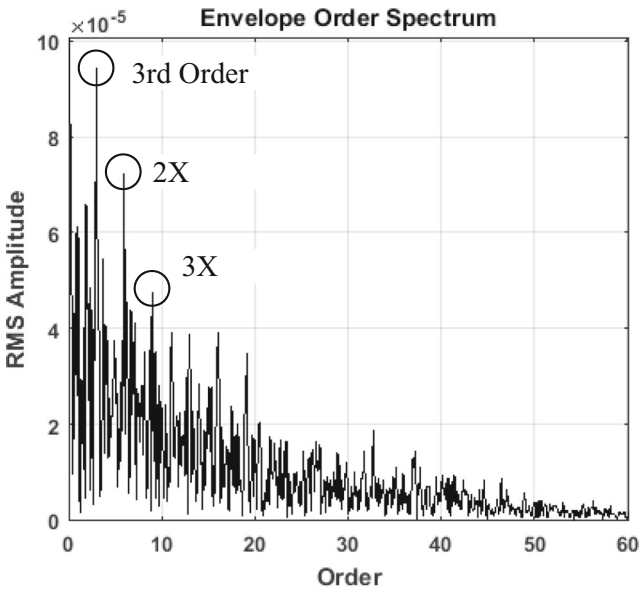

Fig. 20 Envelope order spectrum of the reconstructed signal (Outer race fault)

7.3 Third step

In this step, an envelope order spectrum is applied on the signal obtained from the second step. This clearly reveals the fault order chosen for the simulation, a peak of order 3 with its harmonics, is clearly visible in the spectrum shown in Fig. 14.

8 Application on real measured signals

\In signal processing, simulated signals generally represent an easy challenge for signal processing tools because of their simplicity. In order to prove the efficiency of the proposed method, it will be tested with real signals. For that different signals are measured in the laboratory using two similar faulty bearings, one having an outer race defect, the other having an inner race defect (Fig. 15a), mounted separately on SpectraQuest Machine Fault Simulator (MFS) (Fig. 15b). The MFS is equipped with an automatic and manual speed variator, which allows to measure signals in both stationary and non-stationary case.

8.1 Outer race fault

The first test is performed on a fixed outer race bearing with a defect of order 3.048 situated in the outer race, the speed is varied from 0 to 1800 RPM within 34.13 s as shown in Fig. 16. The speed is measured with a tachometer simultaneously with the vibration signal shown in Fig. 17a, that has been measured with a sampling rate of 15,360 Hz with 524,289 samples. Fig. 17b shows the FFT of the measured signal, it is noticed that the natural frequency is at around 2800 Hz.

The CEEMDAN analysis gives the IMFs shown in Fig. 18. The calculus of the FFT for each IMF shows that the first three IMFs cover the natural frequency, but the appropriate one is IMF2 since it has the most significant kurtosis (38.40).

Using Hilbert transform, the envelope of the chosen IMF has been calculated and then passed through OWMRA to obtain the reconstructed signal shown in Fig. 19. Impacts are visible in the signal, but it is hard to tell whether they correspond to the bearing fault or not before performing order analysis.

After calculating the envelope of the reconstructed signal and then angularly resampling it, the envelope order spectrum is performed, the fault order has been successfully highlighted with the proposed method, which prove its efficiency (Fig. 20).

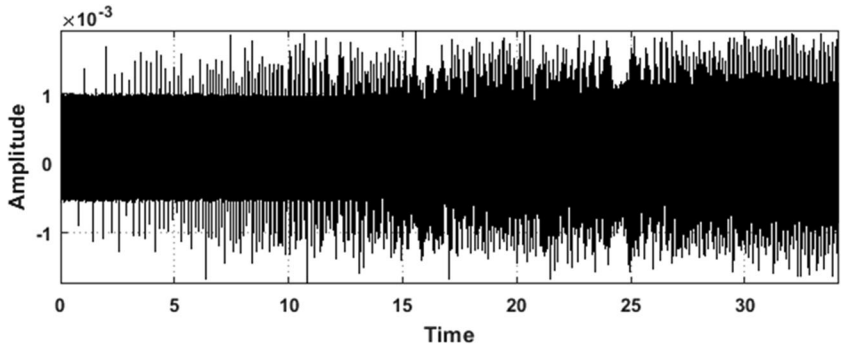

Fig. 21 The measured signal of the bearing with inner race fault

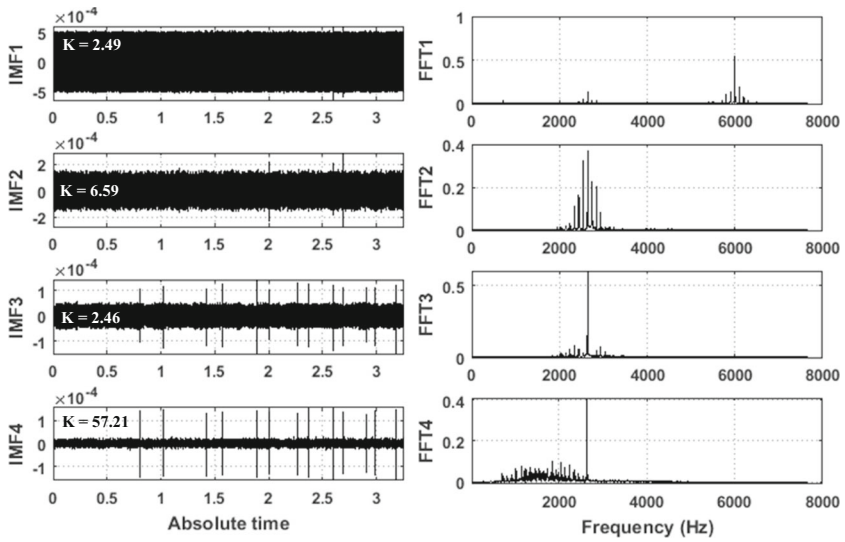

Fig. 22 IMFs of the measured signal with their corresponding FFTs (Inner race fault)

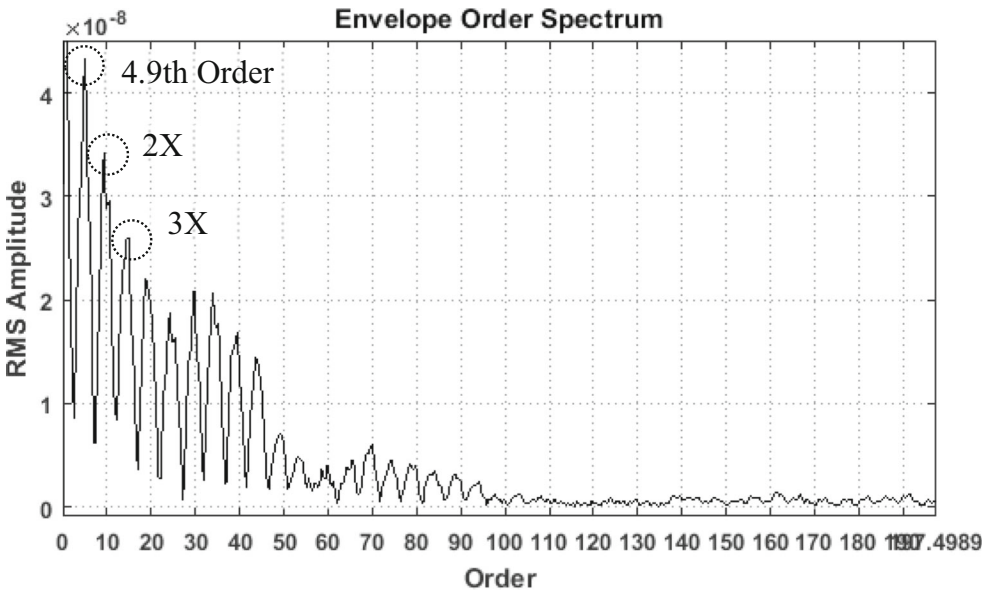

Fig. 23 Envelope order spectrum of the reconstructed signal (Inner race fault)

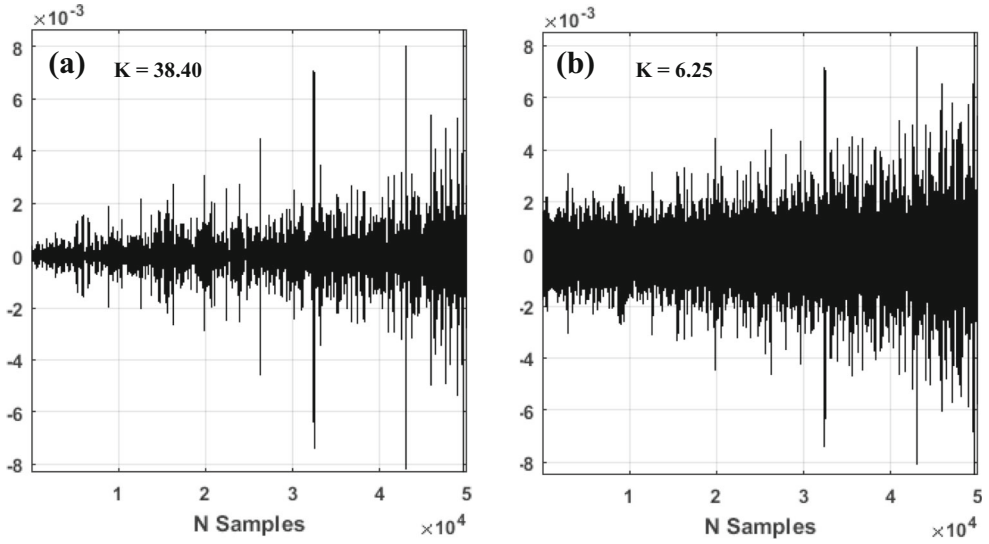

Fig. 24 IMF signal obtained from: (a) CEEMDAN, (b) EEMD

8.2 Inner race fault

The second test has been done with a fixed-outer race bearing, having a defect of order 4.95 on the inner race. The speed profile, the sampling rate and the number of samples are similar to the ones in the previous test. The natural frequency of the second bearing should be also the same (2800 Hz) since the two bearings are similar.

The first remark to be made on the measured signal of Fig. 21 is that the amplitude does not vary so much with the variation of the speed as in the first case (Fig. 17 a) due to modulation phenomenon caused by the relative motion to the defect zone [26–28]. When the fault was steady in the first case, the energy of signal was related to the kinetic energy of the rolling elements, the more the speed rises, the more the energy of the impacts increases. While in the second case, the defect is moving with the rolling elements in a relative motion, which means that the defect has been hit with almost constant force, and the energy of the impacts is the same.

As in the first case, CEEMDAN is used to decompose the measured signal, the obtained IMFs and their corresponding FFTs are shown in Fig. 22. The chosen IMF is number 4 according to the conditions made before, the kurtosis of the 4th IMF reached 57.21, and its spectrum covers the natural frequency. The reconstructed signal obtained after the application of OWMRA and its envelope order spectrum are shown in Fig. 23. The peaks over 4.9th order and its harmonics clearly confirm the presence of the defect in the inner race

9 Results discussion

By the previous results, the efficiency of the proposed method was proved with bearings outer and inner race defects. The

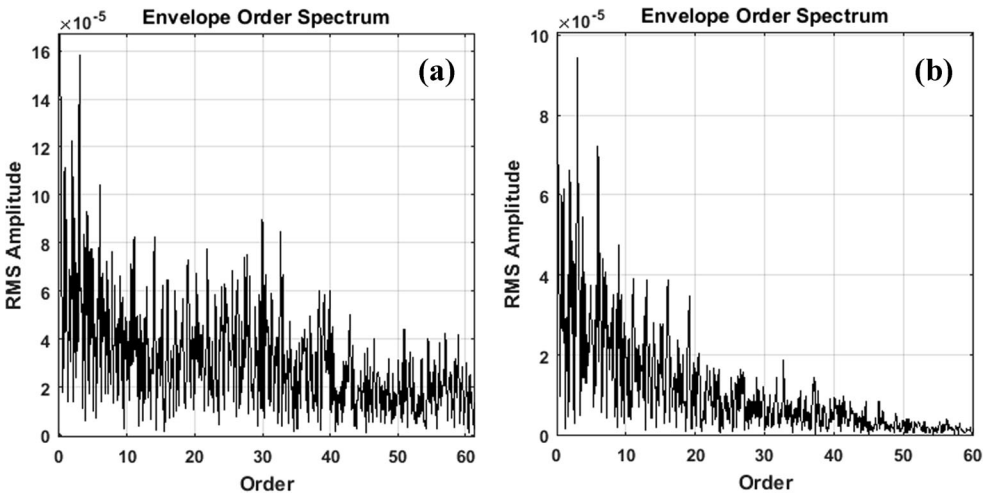

Fig. 25 Envelope Order spectrum obtained after: (a) CEEMDAN, (b) CEEMDAN + WMRA

hybrid approach derives its power from the ability of CEEMDAN in separating the natural oscillatory modes embedded in the non-stationary bearing signal, even when the speed is variable.

In comparison with EEMD, the CEEMDAN algorithm seems better able to extract the series of impulse-like signal components generated by defective bearings. In order to confirm that, the same signal generated from the defective bearing (outer race) used above is analyzed by both EEMD and CEEMDAN algorithms. The second IMF of each result is chosen according to the previously mentioned criterions (Highest Kurtosis, natural frequency coverage).

Notwithstanding that both algorithms were performed on the same signal and with the same number of ensembles, the result is much different as shown in Fig. 24. The CEEMDAN gets clearer impulses visualization than EEMD, this could be supported by the values of kurtosis obtained from each IMF. CEEMDAN gave an IMF with a kurtosis of 38.40, while the IMF given by EEMD had a kurtosis of 6.25 only. The result could be explained by the nature of the adaptive noise added at each stage in CEEMDAN algorithm.

On the other hand, the last result could be less accurate without the use of the OWMRA, since it helps in the isolation of the significant components from the chosen IMF by playing the role of a filter. Figure 25 compares the envelope Order Spectrum obtained after only performing CEEMDAN on the signal of the defective bearing (outer race), with the one obtained after performing both CEEMDAN and WMRA. One can note that the defect order detection is easier using the proposed hybrid method.

10 Conclusion

A hybrid method designed for the detection of rolling bearing faults under variable speed is proposed in this paper. It is based on Complete Empirical Mode Decomposition with Adaptive Noise and an Optimized Wavelet Multi-Resolution Analysis, with the assistance of Order Tracking Analysis. The CEEMDAN is used in order to select the oscillatory mode that best reflect the impulsive form of the defected bearing signal. The OWMRA is then used to filter out the non-significant components from the selected mode envelope and gives a reconstructed signal. The role of OT analysis was to remove the speed variation effects and to help in performing an envelope order spectrum that successfully highlights the characteristic order of the fault. The proposed method is proven to be effective with both simulated and real measured signals. For modern condition monitoring and real time predictive asset management systems, the used hybrid approach could be very helpful when making decisions since it is designed for the surveillance of a critical component that we find in almost every rotating machine, and that works under a non-stationary condition which often represents a challenge for engineers.

Acknowledgments This work was completed in the Laboratory of Mechanics and Structure (LMS) at the University of May 8th 1945, Guelma, Algeria, supported by the Algerian Ministry of Higher Education and Scientific Research (MESRS).

References

1. Randall RB, Antoni J (2011) Rolling element bearing diagnostics—a tutorial. Mech Syst Signal Process 25(2):485–520
2. Capdessus, Cécile, Edgard Sekko, and Jérôme Antoni (2014) "Speed transform, a new time-varying frequency analysis technique." *Advances in Condition Monitoring of Machinery in Non-Stationary Operations*. Springer Berlin Heidelberg, 23–35
3. Sghir KA et al (2013) Vibratory monitoring of a spalling bearing defect in variable speed regime. Mech Industry 14(2):129–136
4. Wu TY, Lai CH, Liu DC (2016) Defect diagnostics of roller bearing using instantaneous frequency normalization under fluctuant rotating speed. J Mech Sci Technol 30(3):1037–1048
5. Wu Z, Huang NE (2009) Ensemble empirical mode decomposition: a noise-assisted data analysis method. Adv Adapt Data Anal 1(01): 1–41
6. Colominas, Marcelo A., et al. "Noise-assisted EMD methods in action." *Advances in Adaptive Data Analysis* 4.04 (2012): 1250025
7. Guo W, Tse Peter W, Djordjevich A (2012) Faulty bearing signal recovery from large noise using a hybrid method based on spectral kurtosis and ensemble empirical mode decomposition. Measurement 45(5):1308–1322
8. Kedadouche, Mourad, Marc Thomas, and Antoine Tahan (2014) "Monitoring machines by using a hybrid method combining MED, EMD, and TKEO." Advances in Acoustics and Vibration 2014
9. Wu TY, Chung YL (2009) Misalignment diagnosis of rotating machinery through vibration analysis via the hybrid EEMD and EMD approach. Smart Mater Struct 18(9):095004
10. Georgoulas G et al (2013) Bearing fault detection based on hybrid ensemble detector and empirical mode decomposition. Mech Syst Signal Process 41(1):510–525
11. Liu X, Lin B, Luo H (2015) Bearing faults diagnostics based on hybrid LS-SVM and EMD method. Measurement 59:145–166
12. Ahn J-H, Kwak D-H, Koh B-H (2014) Fault detection of a roller-bearing system through the EMD of a wavelet denoised signal. Sensors 14(8):15022–15038
13. Djebala A, Babouri MK, Ouelaa N (2015) Rolling bearing fault detection using a hybrid method based on empirical mode decomposition and optimized wavelet multi-resolution analysis. Int J Adv Manuf Technol 79(9–12):2093–2105
14. Mackenzie D (2001) Wavelets: seeing the forest and the trees. Natl Acad Sci
15. Mallat SG (1989) A theory for multiresolution signal decomposition: the wavelet representation. IEEE Trans Pattern Anal Mach Intell 11(7):674–693
16. Djebala A, Ouelaa N, Hamzaoui N (2008) Detection of rolling bearing defects using discrete wavelet analysis. Meccanica 43(3): 339–348
17. Djebala A et al (2012) Application of the wavelet multi-resolution analysis and Hilbert transform for the prediction of gear tooth defects. Meccanica 47(7):1601–1612
18. Pachaud C, Salvetat R, Fray C (1997) Crest factor and kurtosis contributions to identify defects inducing periodical impulsive forces. Mech Syst Signal Process 11(6):903–916

19. Boulenger A, Pachaud C (1998) Diagnostic vibratoire en maintenance préventive. Dunod
20. Fyfe KR, Munck EDS (1997) Analysis of computed order tracking. Mech Syst Signal Process 11(2):187–205
21. Potter Ron, and Mike Gribler (1989) *Computed order tracking obsoletes older methods*. No. 891131. SAE Technical Paper
22. Saavedra PN, Rodriguez CG (2006) Accurate assessment of computed order tracking. Shock Vib 13(1):13–32
23. McFadden PD (1987) A revised model for the extraction of periodic waveforms by time domain averaging. Mech Syst Signal Process 1(1):83–95
24. Antoni J, Randall RB (2002) Differential diagnosis of gear and bearing faults. J Vib Acoust 124(2):165–171
25. Antoni J (2006) The spectral kurtosis: a useful tool for characterizing non-stationary signals. Mech Syst Signal Process 20(2):282–307
26. Rafsanjani A et al (2009) Nonlinear dynamic modeling of surface defects in rolling element bearing systems. J Sound Vib 319(3): 1150–1174
27. Arslan H, Aktürk N (2008) An investigation of rolling element vibrations caused by local defects. J Tribol 130(4):041101
28. Tadina M, Boltežar M (2011) Improved model of a ball bearing for the simulation of vibration signals due to faults during run-up. J Sound Vib 330(17):4287–4301